Published in final edited form as:
Exp Eye Res. 2014 August ; 125: 9–19. doi:10.1016/j.exer.2014.05.014.

Massive formation of square array junctions dramatically alters cell shape but does not cause lens opacity in the cav1-KO mice

Sondip K. Biswas, **Lawrence Brako**, and **Woo-Kuen Lo***
Department of Neurobiology, Morehouse School of Medicine, Atlanta, GA

Abstract

The wavy square array junctions are composed of truncated aquaporin-0 (AQP0) proteins typically distributed in the deep cortical and nuclear fibers in wild-type lenses. These junctions may help maintain the narrowed extracellular spaces between fiber cells to minimize light scattering. Herein, we investigate the impact of the cell shape changes, due to abnormal formation of extensive square array junctions, on the lens opacification in the caveolin-1 knockout mice. The cav1-KO and wild-type mice at age 1 to 22 months were used. By light microscopy examinations, cav1-KO lenses at age 1 to 18 months were transparent in both cortical and nuclear regions, whereas some lenses older than 18 months old exhibited nuclear cataracts. Scanning EM consistently observed the massive formation of ridge-and-valley membrane surfaces in young fibers at approximately 150 μm deep in all cav1-KO lenses studied. In contrast, the typical ridge-and-valleys were only seen in mature fibers deeper than 400 μm in wild-type lenses. The resulting extensive ridge-and-valleys dramatically altered the overall cell shape in cav1-KO lenses. Remarkably, despite dramatic shape changes, these deformed fiber cells remained intact and made close contact with their neighboring cells. By freeze-fracture TEM, ridge-and-valleys exhibited the typical orthogonal arrangement of 6.6 nm square array intramembrane particles and displayed the narrowed extracellular spaces. Immunofluorescence analysis showed that AQP0 C-terminus labeling was significantly decreased in outer cortical fibers in cav1-KO lenses. However, freeze-fracture immunogold labeling showed that the AQP0 C-terminus antibody was sparsely distributed on the wavy square array junctions, suggesting that the cleavage of AQP0 C-termini might not yet be complete. The cav1-KO lenses with nuclear cataracts showed complete cellular breakdown and large globule formation in the lens nucleus. This study suggests that despite dramatic cell shape changes, the massive formation of wavy square array junctions in intact fibers may provide additional adhesive support for maintaining the narrowed extracellular spaces that are crucial for the transparency of cav1-KO lenses.

*Correspondence to: Woo-Kuen Lo, Ph.D., Department of Neurobiology, Morehouse School of Medicine, 720 Westview Dr. SW, Atlanta, GA 30310, Phone: 404-752-1558, Fax: 404-752-1037, wlo@msm.edu.

1. Introduction

Scanning electron microscopy studies have shown that ridge-and-valleys (tongue-and-grooves) belong to one type of interlocking devices regularly observed in deep cortical and nuclear fibers in various species studied, in particular in human and primate lenses [Dickson and Crock, 1972; Kuwabara, 1975; Willekens and Vrensen, 1982; Lo and Harding, 1984; Kuszak et al., 1988]. Freeze-fracture TEM has further demonstrated that ridge-and-valley membrane surfaces are composed of 6.6 nm intramembrane particles arranged in an orthogonal configuration to form wavy square array junctions [Simon et al., 1982; Zampighi et al., 1982; Lo and Harding, 1984; Costello et al., 1985; Lo and Kuck, 1987; Zampighi et al., 1989; Costello et al., 1989]. Our early report [Lo and Harding, 1984] presented the first structural model for the wavy square array junctions that contained contiguous patches of square array intramembrane particles (6.6 nm in size) located alternately in one side of junctional membranes. Since the actual contacts between two contiguous patches of square arrays from two junctional membranes only occur at the sides of the wavy junctions, the junctions thus possess the intramembrane particle-rich and particle-poor areas along the entire junctions [Lo and Harding, 1984]. This unique arrangement of the intramembrane particles in square array junctions has later been confirmed by other laboratories [Costello et al., 1985; 1989; Zampighi et al., 1989]. The wavy square array junctions are thought to play an important role in maintaining the narrowed extracellular spaces between fiber cells to minimize light scattering.

The major protein of square arrays is a truncated water channel protein, aquaporin-0 (AQP0) [Simon et al., 1982; Zampighi et al., 1982; 1989; Costello et al., 1989]. The AQP0, formerly major intrinsic protein (MIP), constitutes approximately 50% of total integral membrane proteins of lens fiber cells in various species studied [Alcala et al., 1975; Horwitz et al., 1979; 1980; Gorin et al., 1984; Takemoto et al., 1986; 1987]. The AQP0 C-terminus undergoes proteolytic cleavages during maturation and aging of fiber cells that result in the formation of a truncated new 22–24 kD molecular weight membrane protein distributed primarily in the deep cortex and nucleus of the lens [Horwitz et al., 1979; Roy et al., 1979; Alcala et al., 1980; Takemoto et al., 1986].

Structurally, freeze-fracture TEM has demonstrated that AQP0 proteins display individual 8–9 nm intramembrane particles randomly distributed in fiber cell membranes of superficial cortical regions [Lo and Harding, 1984; Costello et al., 1985; 1989; Zampighi et al., 1989; Dunia et al., 1998; Zampighi et al., 2003]. Upon proteolytic cleavage, the 8–9 nm AQP0 intramembrane particles are converted into 6.6 nm particles which are arranged into patches of registered square array configuration [Kistler and Bullivant, 1980; Simon et al., 1982; Lo and Harding, 1984; Costello et al., 1985; 1989; Zampighi et al., 1989]. An increased cleavage of AQP0 C-terminus correlates well with the progressive accumulation of square array patches seen in the deep cortex and nucleus as fiber cells age [Simon et al., 1982; Lo and Harding, 1984; Costello et al., 1985; 1989; Zampighi et al., 1989].

In this study, we investigate the impact of the cell shape changes, due to abnormal, massive formation of wavy square array junctions, on the lens opacification in the caveolin-1 knockout mice at age 1 to 22 months. Caveolin-1 is thought to play a role in regulating lipid

transport and has been reported in lens fiber membranes of several species studied [Schubert et al., 2002; Rujoi et al., 2003; Lin et al., 2003; Lo et al., 2004; Sexton et al., 2004; Cenedella et al., 2006; 2007]. Our results showed that in the loss of caveolin-1, wavy square array junctions were extensively formed in young cortical fibers which dramatically altered the overall cell shape. Importantly, these deformed cortical fiber cells still remained intact and made close contacts with their neighboring cells without forming cataract in the cav1-KO lenses at all ages studied. This study suggests that despite significant cell shape changes, the massive formation of wavy square array junctions in intact fibers may provide additional adhesive support for maintaining the narrowed extracellular spaces and compaction that are critical to the transparency of cav1-KO lenses. In addition, it is hypothesized that the loss of caveolin-1 may cause uneven distribution and mobilization of membrane cholesterols in cortical fibers, which may further facilitate the abnormal formation of wavy square array junctions in the cav1-KO lens.

2. Materials and methods

2.1. Animals and lens transparency photography

Caveolin-1 knockout mouse breeders (strain name: STOCK Cav1tm1Mls/J; Stock Number: 004585, homozygotes available with C57B6J background) were purchased from the Jackson Laboratory (Bar Harbor, Maine, U.S.A.). The wild type mouse breeders (Strain Name: B6.Cg-Cav1tm1Mls/J; Stock Number: 007083, heterozygotes available with C57B6J background) were generated and confirmed through a genotypic analysis. The breeding history indicated that the breeders had been back crossed to the 129 strain, followed by outbreeding for 5 generations in the Jackson Laboratory; we have confirmed here that cortical fibers in the cav1-KO lenses contain CP49 beaded filaments by immunofluorescence analysis (data not shown). Both breeders have been under a breeding program at the animal facility of Morehouse School of Medicine. Freshly isolated lenses of cav1−/− mice and cav1+/+ mice at various age intervals (1 month to 22 months old) were collected in PBS solution at RT. They were immediately documented for their transparency under a modified dissecting microscopy system (Nikon SMZ800, Tokyo, Japan) equipped with a lens collecting glass (painted black) and a digital camera (Nikon Coolpix5000, Tokyo, Japan) according to Kuck [Kuck et al., 1981]. After photographing lenses were rapidly fixed in various fixatives for the experiments described below. The animals were treated in accordance with the Association for Research in Vision and Ophthalmology Resolution on the Use of Animals in Research.

2.2. Histology and thin-section electron microscopy

Freshly isolated lenses of cav1-KO mice were fixed in 2.5% glutaraldehyde-0.1 M cacodylate buffer (pH 7.3) for 2 h at room temperature. Each lens was mounted on a specimen holder with superglue and cut into 200 μm slices with a Vibratome (Vibratome 1000 Plus, Ted Pella, Redding, CA). Each lens was oriented on the specimen holder such that either a cross- or longitudinal section of cortical fibers could be obtained. Lens slices were then postfixed in 1% aqueous OsO_4 for 1 h at room temperature, rinsed in distilled water and stained *en bloc* with 0.5% uranyl acetate in 0.15 M NaCl overnight at 4°C. Tissue slices were dehydrated through graded ethanol and propylene oxide, and embedded in

Polybed 812 resin (EMS, Hatfield, PA). Thick sections (1 μm) cut with a diamond knife were stained with 1% toluidine blue and examined with a Zeiss light microscope equipped with a digital camera. Thin sections (80 nm) were cut with a diamond knife, stained with 5% uranyl acetate followed by Reynold's lead citrate and examined in a JEOL 1200EX electron microscope at 80 kV (JEOL, Tokyo, Japan).

2.3. Scanning electron microscopy

Freshly isolated lenses of cav1-KO mice and controls at various ages were fixed in 2.5% glutaraldehyde in 0.1 M cacodylate buffer, pH 7.3 at room temperature for 48–72 h. Each lens was properly orientated and fractured with a needle or sharp razor blade to expose the longitudinal configuration of fiber cells in the entire lens. Lens halves were then postfixed in 1% aqueous OsO_4 for 1–2 h at room temperature, dehydrated in graded ethanol and dried in a Samdri-795 critical point dryer (Tousimis Inc., Rockville, MD). Lens halves were oriented and mounted on specimen stubs and coated with gold/palladium in a Hummer VII sputter coater (Anatech, Union City, CA). Micrographs were taken with a JEOL 820 scanning electron microscope at 10 kV.

2.4. Freeze-fracture TEM

Our routine procedures were used in this study [Biswas and Lo, 2007]. In brief, freshly isolated lenses of cav1-KO mice and controls were fixed in 2.5% glutaraldehyde in 0.1M cacodylate buffer (pH 7.3) at RT for 2–4 hours. After washing in buffer, lenses were orientated to obtain sagittal (longitudinal) sections with a Vibratome and tissue slices were collected, marked serially from superficial to deep and kept separately. The slices were then cryoprotected with 25% glycerol in 0.1 M cacodylate buffer at RT for 1 hour. A single lens slice was mounted on a gold specimen carrier and frozen rapidly in liquefied Freon 22 and stored in liquid nitrogen. Cryofractures of frozen slices were made in a modified Balzers 400T freeze-fracture unit, at a stage temperature of −135°C in a vacuum of approximately 2×10^{-7} Torr. The lens tissue was fractured by scraping a steel knife across its frozen surface to expose fiber cell membranes. The fractured surface was then immediately replicated with platinum (~2 nm thick) followed by carbon film (~25 nm thick). The replicas, obtained by unidirectional shadowing at 45° angle, were cleaned with household bleach and examined with a JEOL 1200EX TEM.

2.5. Freeze-fracture replica immunogold labeling (FRIL)

We followed our previous procedures [Biswas et al., 2009]. Briefly, freshly isolated cav1-KO and WT mouse lenses were lightly fixed in 0.75% paraformaldehyde in PBS for 30–45 min at RT, and then cut into 300 μm slices with a Vibratome to make freeze-fracture replicas. One drop of 0.5% parloidion in amyl acetate was used to secure the integrity of the whole piece of a large replica during cleaning and immunogold labeling procedures. The replica was digested with 2.5% sodium dodecyl sulfate, 10 mM Tris-HCl, 30mM sucrose, pH 8.3 (SDS buffer) at 50°C until all visible attached tissue debris was removed from the replica. The replica was then rinsed with PBS, blocked with 4% BSA-0.5% teleostean gelatin in PBS for 30 min and incubated with the rabbit AQP0-loop polyclonal antibody [Johnson et al., 1991] (a gift from Ross Johnson of University of Minnesota, Minneapolis, MN; Purified rabbit Ab #7803 to peptide corresponding to positions 105–125 in bovine

MIP26) at 1:10 dilution with the blocking solution, and the rabbit anti-AQP0 polyclonal antibody made from the C-terminus (Alpha Diagnostic International, San Antonio, TX) at 1:10 dilution for 1 h at RT. The replica was washed with PBS and incubated with 10 nm Protein A gold (EY Laboratories, San Mateo, CA) at 1:50 dilution for 1 h at RT. After rinsing, the replica was fixed in 0.5% glutaraldehyde in PBS for 10 min, rinsed in water, collected on a 200-mesh Gilder finder grid (EMS, Hatfield, PA), rinsed with 100% amyl acetate for 30 s to remove parloidion and viewed with a JEOL 1200EX TEM.

2.6. Immunofluorescence labeling of AQP0 antibodies

Freshly isolated lenses of cav1-KO and WT mice were fixed in 4% paraformaldehyde-PBS (pH 7.3) for overnight at 4°C, and washed for 2 × 30 min in PBS, infiltrated in 0.6 M sucrose-PBS for overnight at 4°C, and transferred to 1.15 M sucrose-PBS for another overnight at 4°C. Lenses were embedded in OCT in plastic embedding molds for 2 h at RT and then frozen in liquid nitrogen. Cryosectioning of thick sections (20 μm thick) was done with a cryostat at −20°C. Frozen sections containing cortical and nuclear fibers were collected with ambient-temperature pre-coated glass slides, and stored in a −80°C freezer. The frozen section slides were later transferred to a −20°C freezer for overnight before use. For antibody labeling, frozen sections were immersed in −20°C acetone for 2 min, washed in PBS at RT for 2 × 10 min, and blocked in 2% BSA-PBS blocking solution for 1 h at RT. Lens sections were then incubated with the rabbit AQP0 C-terminus polyclonal antibody (Alpha Diagnostic International, San Antonio, TX) at 1:200 dilution, and the rabbit AQP0-loop polyclonal antibody [Johnson et al., 1991] (a gift from Ross Johnson of University of Minnesota, Minneapolis, MN; Purified rabbit Ab #7803 to peptide corresponding to positions 105–125 in bovine MIP26) at 1:200 dilution in the blocking solution for 2 h at RT. After washed in PBS for 2 × 10 min, lens sections were incubated with FITC-conjugated goat anti-rabbit IgG secondary antibody at 1:200 dilutions (Jackson ImmunoResearch Laboratories, West Grove, PA) for 1 h at RT, rinsed in PBS, mounted with anti-photobleaching medium and examined with an Olympus confocal microscope.

2.7. Cytochemical detection of membrane cholesterol in flat membranes and wavy aquaporin junctions

We followed our routine procedures [Biswas et al., 2009]. Briefly, vibratome slices of wild-type controls and cav1-KO mice were incubated in a mixture of 2.5% glutaraldehyde in 0.1 M cacodylate buffer and 0.1% filipin in dimethyl formamide (Sigma, St. Louis, MO) for 24 h at RT. We used freshly prepared filipin solution in each experiment to ensure the best quality control for consistent results. The slices were then cryoprotected with 25% glycerol in 0.1 M cacodylate buffer at RT for 1 h and processed for conventional freeze-fracture TEM described above. The filipin-cholesterol-complexes (FCCs) are discrete particles or pits (25–35 nm in diameter) which can be clearly visualized on the P face and E face of the plasma membrane with freeze-fracture TEM. The formation of FCCs is due to the polyene antibiotic filipin reacting specifically with membrane cholesterol which produces characteristic membrane lesions seen as the FCCs.

Quantitative analysis was carried out to determine whether there were significant changes in the amounts of the cholesterol complexes FCCs in areas of flat fiber cell membranes in the

cav1-KO lenses. The micrographs at 30,000X were taken randomly from flat cell membranes in the outer cortex from three replicas prepared from three different animals of similar ages. Each membrane area (μm^2) was measured with the Zeiss AxioVision LE 4.4 on PC, and the number of FCCs per unit membrane was counted manually with a cell counter. The number of FCCs per μm^2 membrane area was calculated to determine the cholesterol-rich area vs. cholesterol poor area. Statistical comparisons of the mean percentage of cholesterol-rich vs. cholesterol-poor areas were made by T-test using the software SPSS 14.0 (SPSS Inc.). A $P<0.05$ was considered significant.

3. Results

3.1. Lens transparency in the cav1-KO mice

By using the dissecting light microscopy system (see Methods) modified from Kuck [Kuck et al., 1981], all freshly isolated lenses showed transparency in both cortical and nuclear core regions of the cav1-KO lenses at age 1 to 18 months examined (Fig. 1A–C). However, some lenses at age 19 to 22 months displayed nuclear cataract and the cataract was often shown only in one of the lens pair (Fig. 1D). Lenses from wild-type mice at all ages examined were all transparent (data not shown).

3.2. Changes in cell shape and membrane surface of cortical fibers in cav1-KO lenses

Scanning electron micrographs of the wild-type and cav1-KO lenses at low magnification showed that they displayed similarity in overall intact structural configurations (Fig. 2A–D). Figure 3 illustrates the structural configurations of fiber cells with normal sizes and shapes in different regions from 50 to 600 μm deep in a one-month-old wild-type lens. While typical interlocking protrusions were distributed abundantly in cortical fibers from 50 to 300 μm deep, the distinct ridge-and-valley membrane surfaces were distributed mainly in the deep cortical fibers from 400 to 600 μm deep (Fig. 3A–F). Similar ridge-and-valleys were also distributed regularly in the nuclear fiber cells (data not shown).

In contrast, several significant changes were observed in a one-month-old cav1-KO lens (Fig. 4A–F). The superficial cortical fiber cells significantly increased their sizes and altered shapes. The most dramatic change was the massive formation of wavy ridge-and-valley membrane surfaces in the cortical fibers at approximately 150 μm deep toward the deep cortex (Fig. 4B–E). The resulting extensive ridge-and-valley membrane surfaces dramatically altered the overall cell shape. Remarkably, despite the significant cell shape changes, these deformed fiber cells still remained intact and made close contact with their neighboring cells (Fig. 4B–E).

3.3. Similarity of extensive ridge-and-valleys in inner cortical fibers of cav1-KO lenses at different ages

We compared the ridge-and-valleys surface patterns of cortical fibers at 400 μm deep among cav1-KO lenses of different ages to evaluate their structural characteristics in relation to the transparency (Fig. 5A–D). All ridge-and-valleys exhibited the extreme similarity of surface structural features in all ages examined, including those of the 19 and 22 months old with nuclear cataracts (Fig. 5C, D). The narrowed extracellular space between the ridge-and-

valleys (square array junctions) of adjacent fiber cells was clearly demonstrated in the thin-section electron micrograph (Fig. 5E). This indicates that the abnormal formation of extensive square array junctions does not cause lens opacification.

Rather, the development of nuclear cataract in the cav1-KO lens at age 19 months was due to complete breakdown of nuclear fibers and the formation of numerous large globules in the lens core (Fig. 6A, B). It is not known what causes the cell breakdown and formation of extensive globules in the aging lens nucleus. Since the nuclear cataract was not regularly found in all cav1-KO lenses older than 18 months old, the loss of caveolin-1 alone might not be the main factor for nuclear cataract formation in these aging mice.

3.4. Intramembrane structures of AQP0-dependant wavy square array junctions in cortical fiber cells of cav1-KO lenses

Freeze-fracture TEM revealed the undulating ridge-and-valley surface patterns typically arranged in parallel bundles in outer cortical fibers of cav1-KO lenses (Fig. 7A). At high magnification, patches of square array intramembrane particles (6.6 nm) were identified as the major intramembrane structure of wavy ridge-and-valleys in the cav1-KO lens (Fig. 7B, C). The 6.6 nm small intramembrane particles (p-face) or pits (e-face) were regularly arranged into contiguous patches of the orthogonal configuration along the sides of wavy square array junctions (Fig. 7B, C). The narrowed intercellular spaces between the wavy square array junctions were observed concurrently between the p-face and the e-face of the junction membranes (Fig. 7B, C). A number of large intramembrane particles (8–9 nm) were also distributed along these newly-formed wavy square array junctions (Fig. 7B, C).

Since truncations of AQP0 C-termini occurred prematurely in cortical fibers in cav1-KO lenses (see Fig. 8), freeze-fracture immunogold labeling (FRIL) was used to validate the high resolution localization of AQP0 proteins in wavy square array junctions. FRIL showed that 10-nm gold particles representing the AQP0-loop antibody were localized mostly along the wavy square array membranes (Fig. 7D). In contrast, the AQP0 C-terminus antibody was only sparsely distributed along the valleys or the sides of wavy square array membranes (Fig. 7E). The contiguous square array membrane particles were observed at the sides of the wavy junctions (Fig. 7E).

3.5. Changes on immunofluorescence labeling of AQP0 in cav1-KO and WT lenses

Confocal immunofluorescence labeling of AQP0 was used to determine at low magnification overview whether changes occurred in the cav1-KO lens during massive formation of square array junctions in the outer and inner cortical regions. Figure 8 shows that AQP0 C-terminus antibody labeled the major lens cortex (approximately 300 μm deep) in the wild-type lens (Fig. 8A). In contrast, labeling of the AQP0 C-terminus antibody was restricted in the superficial and outer cortical fibers within approximately 150 μm deep in the cav1-KO lens (Fig. 8B). However, the AQP0-loop antibody was positively labeled in the entire cortical fibers in the cav1-KO lens (Fig. 8C), suggesting that the premature cleavage of AQP0 C-terminus occurred in the outer and inner cortical fibers in the cav1-KO lenses.

3.6. Changes on membrane cholesterol in flat membranes and wavy square array junctions in cav1-KO lenses

Since caveolin-1 is known to play a role in regulating lipid transport [Schubert et al., 2002; Lo et al., 2004; Cenedella et al., 2007], a possible change in membrane cholesterol distribution in the cav1-KO lenses was examined with filipin cytochemistry and freeze-fracture TEM. Freeze-fracture TEM showed that membrane particle free areas were frequently observed in outer cortical fiber cells in cav1-KO lenses (Fig. 9A, B), suggesting that cholesterol may be distributed more richly in these membrane particle-free areas. Filipin cytochemical analysis showed that uneven distributions of FCCs (represented by 25–35 nm filipin-cholesterol-complex particles or pits) were frequently found in various cell membrane areas of cortical fibers (Fig. 9C, D). The filipin-cholesterol-complexes (FCCs) are discrete particles or pits (25–35 nm in diameter) which can be clearly visualized on the p-face and e-face of the plasma membrane with freeze-fracture TEM. Our quantitative estimations showed that the amounts of membrane cholesterol per μm^2 area between FCC-rich and FCC-poor area were considerably different (Fig. 9C, D). The ratio of cholesterol between the areas of cholesterol-poor (359 FCC/μm^2) and cholesterol-rich (1031 FCC/μm^2) is approximately 1:3. In addition, newly formed square array junctions displayed uneven distributions of membrane cholesterols along the wavy junctions (Fig. 9E, F). The FCC cholesterol particles were typically not associated with the square array junctions at the sides (Fig. 9E) or the valley regions where the square array intramembrane particles (p-face) were heavily accumulated (Fig. 9F). In the control experiments, the distinct uneven distributions of membrane particle free areas were not found in the wild-type lens (data not shown).

4. Discussion

This study shows that despite the dramatic alterations of cell shape due to massive formation of square array junctions, all cortical fibers still retain their transparency in the cav1-KO lens. This result suggests that the lens transparency can be maintained if the fiber cells are intact and the extracellular spaces are kept narrow by the extensive square array junctions. The presence of the deformed intact cortical fiber cells with their narrowed extracellular spaces in the cav1-KO lenses is demonstrated in SEM, thin-section TEM and freeze-fracture TEM (Fig. 4, 5 and 7). Thus, it is very conceivable that the massive formation of wavy square array junctions in deformed intact fibers may provide extra adhesion support for maintaining the narrowed extracellular spaces that are critical to the transparency of cav1-KO lenses. In this respect, the present study is in good agreement with an early work of Yoon et al [Yoon et al., 2008], which concludes that long-range structural order in the lens is a requirement for optical clarity. In contrast, breakdown of nuclear fiber cells and the formation of many large globules cause the development of nuclear cataracts seen in some cav1-KO lenses older than 18 months old (Fig. 1, 6). Although it is not known what causes the cell breakdown and formation of extensive globules in the aging lens nucleus, the loss of caveolin-1 alone may not be the sole factor for the cataract formation because the nuclear cataract was not regularly found in all cav1-KO lenses older than 18 months old.

This study reveals that the formation process of square array junctions in the cav1-KO lenses is similar to those described in the human lens [Lo and Harding, 1984] and other

species [Costello et al., 1985; 1989; Zampighi et al., 1989]. It has been reported that the formation of square array junctions is directly associated with the proteolytic cleavage of the C-terminus of AQP0 in deep cortex and nucleus [Kistler and Bullivant, 1980; Zampighi et al., 1982; Costello et al., 1985; 1989; Zampighi et al., 1989; Michea et al., 1995]. Structurally, there is a transformation from the individual 8–9 nm AQP0 intramembrane particles into the clusters of 6.6 nm intramembrane particles arranged in the orthogonal (square array) configuration [Kistler and Bullivant, 1980; Zampighi et al., 1982; Simon et al., 1982; Lo and Harding, 1984; Costello et al., 1985; Costello et al., 1989; Zampighi et al., 1989]. In this study, immunofluorescence study has indeed detected the premature cleavage of AQP0 C-terminus in the outer cortical fibers in cav1-KO lenses (Fig. 8B). Nevertheless, immunogold labeling at the electron microscopic level has shown that there is sparse distribution of AQP0 C-terminus in the square array junctions (Fig. 7E). This indicates that the truncation of AQP0 C-termini has not yet completed during the massive formation of wavy square array junctions in the cav1-KO lens. Furthermore, differences in the square array structures are also observed between the cav1-KO lenses and the normal aging lenses. For example, many individual 8–9 nm intramembrane particles are still regularly distributed along the wavy square array junctions in the cav1-KO lenses (Fig. 7B, C). The nature of these particles is not known. They may represent the individual 8–9 nm AQP0 whole molecules that have not yet converted into the 6.6 nm square array particles in the newly formed junctions [Lo and Harding, 1984; Zampighi et al., 1989]. Another possibility is that some of those 8–9 nm intramembrane particles are of the other integral membrane proteins in cortical fiber cells.

It is not known why the loss of caveolin-1 causes massive formation of square array junctions in cav1-KO lens. Caveolin-1 is present in the lens and has been shown to play a role in regulating the lipid transport in various cell types [Schubert et al., 2002; Lin et al., 2003; Rujoi et al., 2003; Lo et al., 2004; Sexton et al., 2004; Cenedella et al., 2006; Cenedella et al., 2007]. It is postulated that the loss of caveolin-1 may cause uneven transport and mobilization of lipids within the fiber cell membrane, since the present study reveals uneven distributions of membrane cholesterol in cortical fiber cells of the cav1-KO lenses (Fig. 9). The uneven mobilization of membrane cholesterol may further facilitate an unequal distribution (mobilization) of AQP0 membrane particles for the formation of wavy square array junctions. It is known that the wavy square array junctions are composed of asymmetrical distributions of the AQP0 protein and lipid in the valley portion vs. the ridge portion of the junctions [Lo and Harding, 1984; Costello et al., 1989; Zampighi et al., 1989]. Our filipin cytochemistry analysis has shown that there are asymmetrical distributions of cholesterol and square array particles in the wavy square array junctions (Fig. 9).

In conclusion, this study supports the functional roles of wavy square array (aquaporin) junctions in maintaining the narrowed extracellular spaces and transparency in deformed intact fiber cells of the cav1-KO lens. It is also evidenced that cellular breakdown and globulization of nuclear fiber cells are the cause of the late-onset nuclear cataract seen in some aging cav1-KO mice. The cav1-KO mouse may serve as an ideal animal model for investigating the adhesion function of AQP0 and wavy aquaporin junctions in the lens.

Acknowledgments

The authors thank Ross Johnson of University of Minnesota, Minneapolis, MN for providing purified AQP0 pAb (whole) and AQP0 pAb (loop) antibodies, and Michael Elliott of the Dean McGee Eye Institute, University of Oklahoma for supplying cav1-KO and wild-type lenses for the initial phase of this study. This study was supported by NEI/NIH grant EY05314 to W.K.L. and Grant RR03034 from the Research Centers in Minority Institutions, National Center for Research Resources, National Institutes of Health (Morehouse School of Medicine).

References

Alcala J, Lieska N, Maisel H. Protein composition of bovine lens cortical fiber cell membranes. Exp Eye Res. 1975; 21:581–95. [PubMed: 1204686]

Alcala J, Putt D, Maisel H. Limited proteolysis of gap junction protein is intrinsic in mammalian lens fiber-cell plasma membranes. Biochem Biophys Res Commun. 1987; 147:846–53. [PubMed: 3115266]

Alcala J, Valentine J, Maisel H. Human lens fiber cell plasma membranes. I. Isolation, polypeptide composition and changes associated with ageing. Exp Eye Res. 1980; 30:659–77. [PubMed: 7418744]

Biswas SK, Jiang JX, Lo WK. Gap junction remodeling associated with cholesterol redistribution during fiber cell maturation in the adult chicken lens. Mol Vis. 2009; 15:1492–508. [PubMed: 19657477]

Biswas SK, Lo WK. Gap junctions contain different amounts of cholesterol which undergo unique sequestering processes during fiber cell differentiation in the embryonic chicken lens. Mol Vis. 2007; 13:345–59. [PubMed: 17392685]

Cenedella RJ, Neely AR, Sexton P. Multiple forms of 22 kDa caveolin-1 alpha present in bovine lens cells could reflect variable palmitoylation. Exp Eye Res. 2006; 82:229–35. [PubMed: 16125174]

Cenedella RJ, Sexton PS, Brako L, Lo WK, Jacob RF. Status of caveolin-1 in various membrane domains of the bovine lens. Exp Eye Res. 2007; 85:473–81. [PubMed: 17669400]

Costello MJ, McIntosh TJ, Robertson JD. Membrane specializations in mammalian lens fiber cells: distribution of square arrays. Curr Eye Res. 1985; 4:1183–201. [PubMed: 4075818]

Costello MJ, McIntosh TJ, Robertson JD. Distribution of gap junctions and square array junctions in the mammalian lens. Invest Ophthalmol Vis Sci. 1989; 30:975–89. [PubMed: 2722452]

Dickson DH, Crock GW. Interlocking patterns on primate lens fibers. Invest Ophthalmol. 1972; 11:809–15. [PubMed: 4627255]

Dunia I, Recouvreur M, Nicolas P, Kumar N, Bloemendal H, Benedetti EL. Assembly of connexins and MP26 in lens fiber plasma membranes studied by SDS-fracture immunolabeling. J Cell Sci. 1998; 111(Pt 15):2109–20. [PubMed: 9664032]

Gorin MB, Yancey SB, Cline J, Revel JP, Horwitz J. The major intrinsic protein (MIP) of the bovine lens fiber membrane: characterization and structure based on cDNA cloning. Cell. 1984; 39:49–59. [PubMed: 6207938]

Horwitz J, Robertson NP, Wong MM, Zigler JS, Kinoshita JH. Some properties of lens plasma membrane polypeptides isolated from normal human lenses. Exp Eye Res. 1979; 28:359–65. [PubMed: 436982]

Johnson KR, Sas DF, Johnson RG. MP26, a protein of intercellular junctions in the bovine lens: electrophoretic and chromatographic characterization. Exp Eye Res. 1991; 52:629–39. [PubMed: 2065732]

Kistler J, Bullivant S. Lens gap junctions and orthogonal arrays are unrelated. FEBS Lett. 1980; 111:73–8. [PubMed: 7358167]

Kuck JF, Kuwabara T, Kuck KD. The Emory mouse cataract: an animal model for human senile cataract. Curr Eye Res. 1981; 1:643–9. [PubMed: 7346236]

Kuszak JR, Ennesser CA, Umlas J, sai-Kaplan MS, Weinstein RS. The ultrastructure of fiber cells in primate lenses: a model for studying membrane senescence. J Ultrastruct Mol Struct Res. 1988; 100:60–74. [PubMed: 3209860]

Kuwabara T. The maturation of the lens cell: a morphologic study. Exp Eye Res. 1975; 20:427–43. [PubMed: 1126408]

Lin D, Zhou J, Zelenka PS, Takemoto DJ. Protein kinase Cgamma regulation of gap junction activity through caveolin-1-containing lipid rafts. Invest Ophthalmol Vis Sci. 2003; 44:5259–68. [PubMed: 14638725]

Lo WK, Harding CV. Square arrays and their role in ridge formation in human lens fibers. J Ultrastruct Res. 1984; 86:228–45. [PubMed: 6544861]

Lo WK, Kuck JF. Alterations in fiber cell membranes of Emory mouse cataract: a morphologic study. Curr Eye Res. 1987; 6:433–44. [PubMed: 3581865]

Lo WK, Zhou CJ, Reddan J. Identification of caveolae and their signature proteins caveolin 1 and 2 in the lens. Exp Eye Res. 2004; 79:487–98. [PubMed: 15381033]

Michea LF, Andrinolo D, Ceppi H, Lagos N. Biochemical evidence for adhesion-promoting role of major intrinsic protein isolated from both normal and cataractous human lenses. Exp Eye Res. 1995; 61:293–301. [PubMed: 7556493]

Roy D, Spector A, Farnsworth PN. Human lens membrane: comparison of major intrinsic polypeptides from young and old lenses isolated by a new methodology. Exp Eye Res. 1979; 28:353–8. [PubMed: 436981]

Rujoi M, Jin J, Borchman D, Tang D, Yappert MC. Isolation and lipid characterization of cholesterol-enriched fractions in cortical and nuclear human lens fibers. Invest Ophthalmol Vis Sci. 2003; 44:1634–42. [PubMed: 12657603]

Schubert AL, Schubert W, Spray DC, Lisanti MP. Connexin family members target to lipid raft domains and interact with caveolin-1. Biochemistry. 2002; 41:5754–64. [PubMed: 11980479]

Sexton PS, Neely AR, Cenedella RJ. Distribution of caveolin-1 in bovine lens and redistribution in cultured bovine lens epithelial cells upon confluence. Exp Eye Res. 2004; 78:75–82. [PubMed: 14667829]

Simon SA, Zampighi G, McIntosh TJ, Costello MJ, Ting-beall HP, Robertson JD. The structure of junctions between lens fiber cells. Biosci Rep. 1982; 2:333–41. [PubMed: 7093443]

Takemoto L, Takehana M, Horwitz J. Covalent changes in MIP26K during aging of the human lens membrane. Invest Ophthalmol Vis Sci. 1986; 27:443–6. [PubMed: 3949474]

Willekens B, Vrensen G. The three-dimensional organization of lens fibers in the rhesus monkey. Graefes Arch Clin Exp Ophthalmol. 1982; 219:112–20. [PubMed: 7173625]

Yoon KH, Blankenship T, Shibata B, FitzGerald PG. Resisting the effects of aging: a function for the fiber cell beaded filament. Invest Ophthalmol Vis Sci. 2008; 49:1030–6. [PubMed: 18326727]

Zampighi G, Simon SA, Robertson JD, McIntosh TJ, Costello MJ. On the structural organization of isolated bovine lens fiber junctions. J Cell Biol. 1982; 93:175–89. [PubMed: 7068755]

Zampighi GA, Hall JE, Ehring GR, Simon SA. The structural organization and protein composition of lens fiber junctions. J Cell Biol. 1989; 108:2255–75. [PubMed: 2738093]

Zampighi GA, Kreman M, Lanzavecchia S, Turk E, Eskandari S, Zampighi L, Wright EM. Structure of functional single AQP0 channels in phospholipid membranes. J Mol Biol. 2003; 325:201–10. [PubMed: 12473462]

Highlights

This paper demonstrates that the lens transparency can be maintained for a long period of time even under the conditions that the fiber cell shapes are dramatically altered.

Importantly, however, the prerequisites are that the cells need to be intact and their extracellular spaces be kept narrow. In the case of caveolin-1 knockout lens in this study, the narrowed extracellular spaces between deformed intact cortical fiber cells are maintained by the abnormal, massive formation of square array junctions. These junctions are believed to play an important adhesion role in maintaining the narrowed extracellular spaces between fiber cells to minimize light scattering in the normal lens.

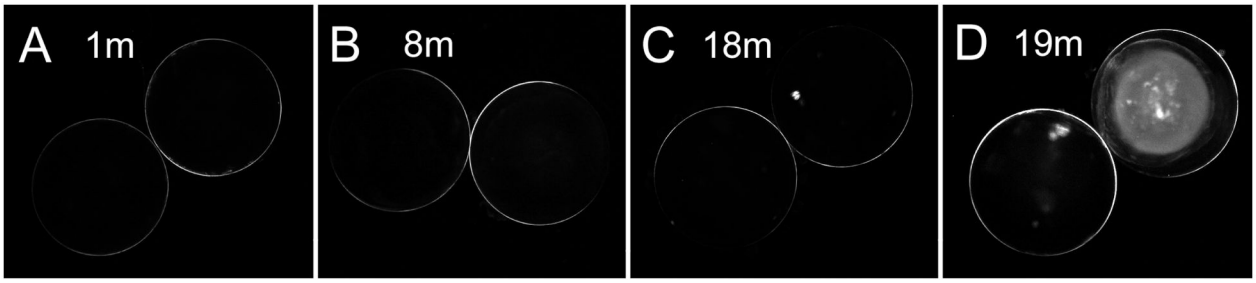

Figure 1.

Representative photographs of lens transparency in cav1-KO mice at different ages. All lenses examined in cav1-KO mice at age 1 to 18 months are transparent. A–C show transparent lenses at 1 month, 8 months and 18 months of age. Some lenses at 19 months and older display nuclear cataracts with various densities in the cav1-KO mice (D).

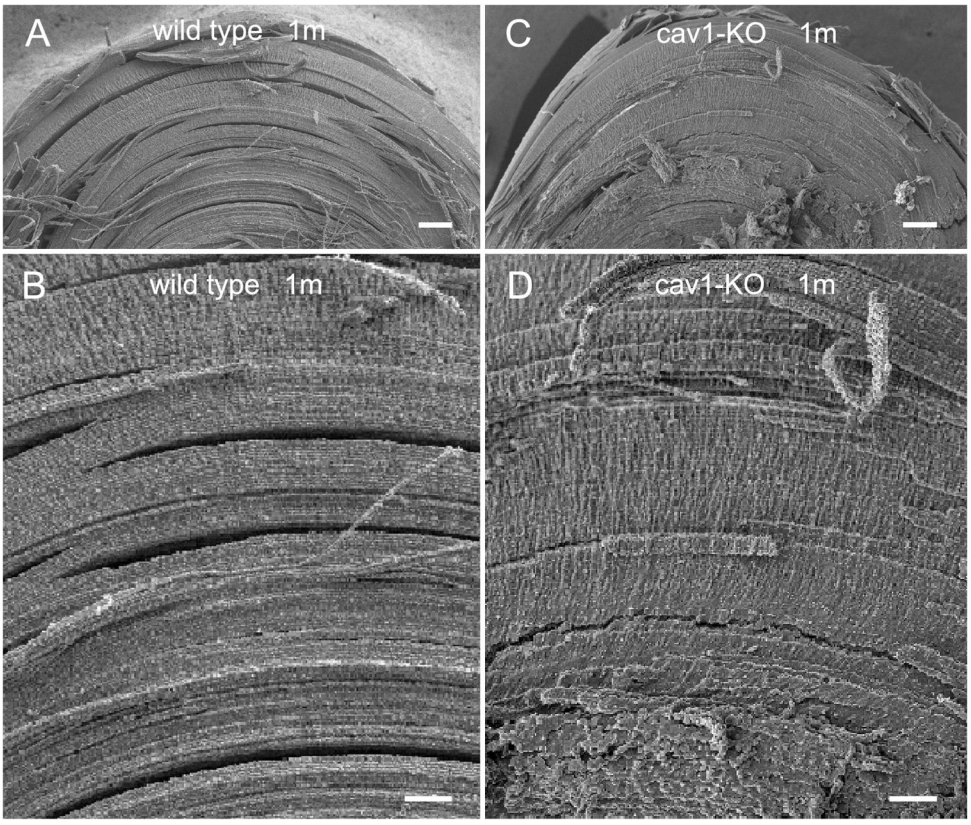

Figure 2.

SEM comparison of intact cortical fibers in wild-type and cav1-KO lenses at low magnifications. The similarity in structural compactness between intact cortical fibers of wild-type (A and B) and cav1-KO (C and D) is discernible at the low magnification micrographs. Scale bars: A and C= 100 μm; B and D=50 μm.

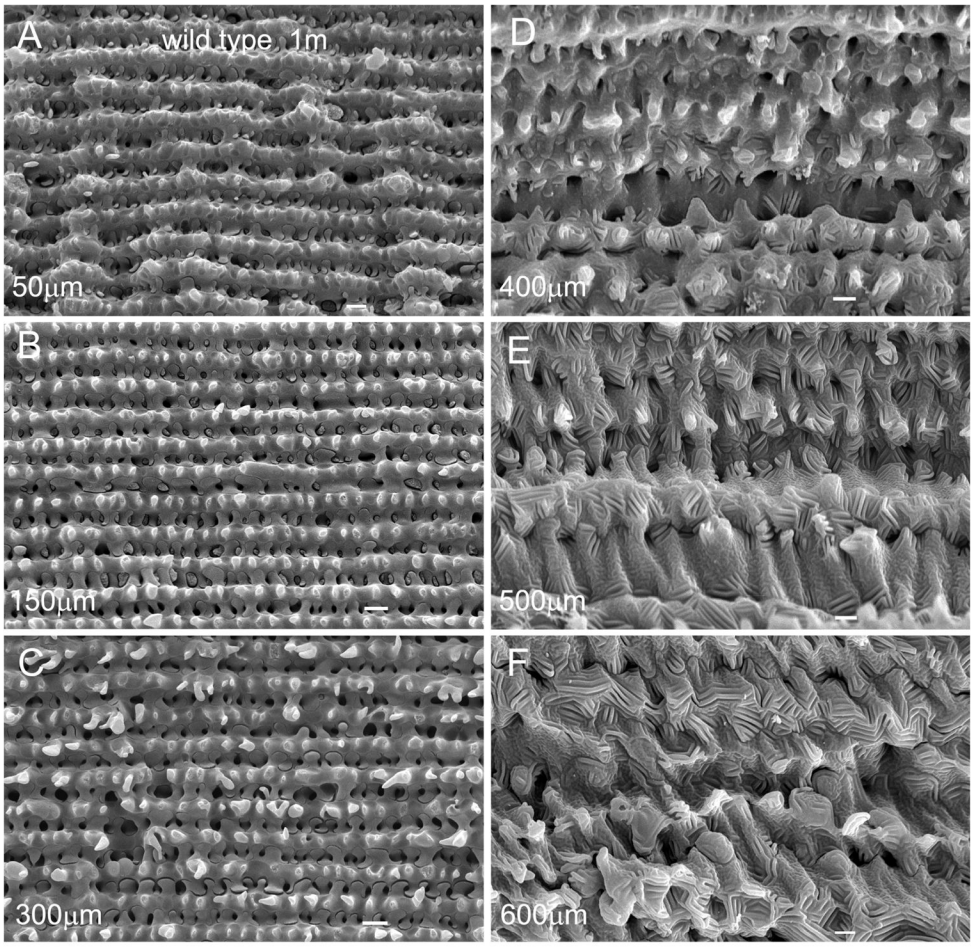

Figure 3.

Normal cell shape and membrane surface of cortical fibers in wild-type lenses. The cell membranes of normal cortical fiber cells change gradually from the smooth surface in the superficial cortex (A) to more irregular surface with elaborate interlocking protrusions in the outer cortex (B, C), approximately from 50 μm to 300 μm deep from the equatorial lens surface. The ridge-and-valley surface patterns, which represent wavy aquaporin junctions of fiber cells, are first seen in the inner cortex (D), approximately 400 μm deep from the lens surface. These ridge-and-valley surface patterns are found extended toward the entire deep cortical regions (i.e., 600 μm deep) of the lens (E, F). Scale bars: A–F = 1 μm.

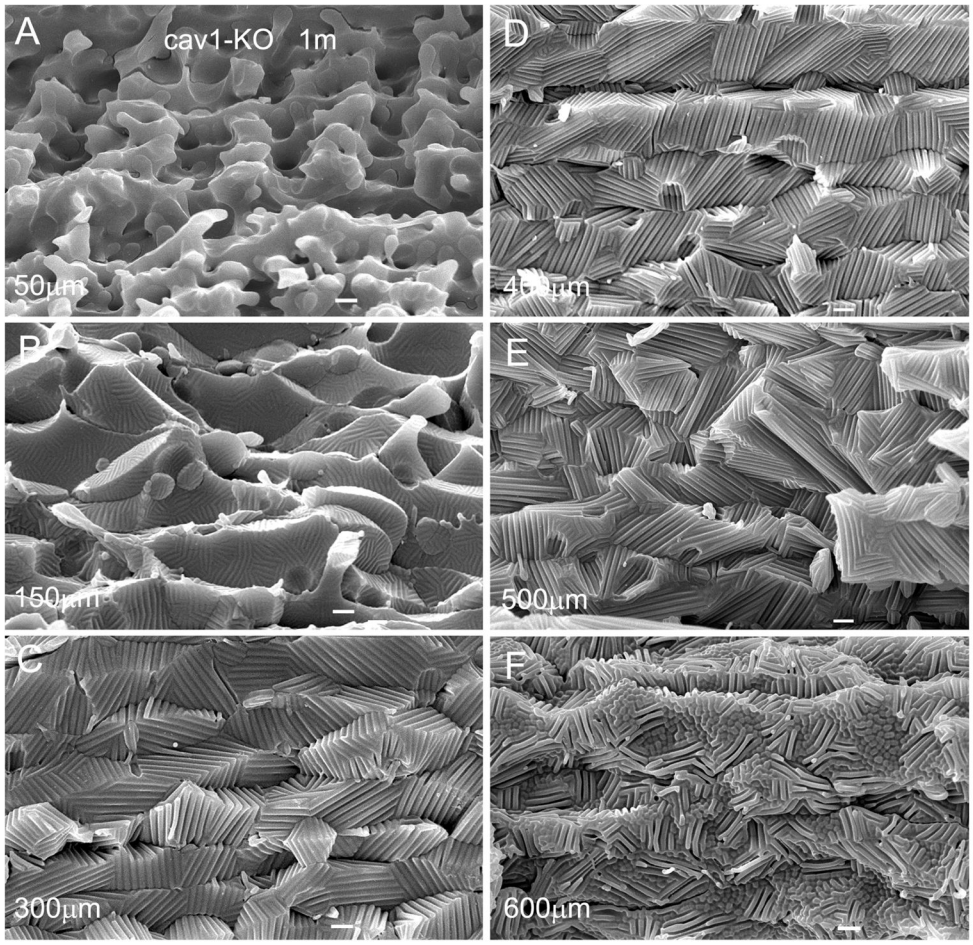

Figure 4.

Changes in cell shape and membrane surface of cortical fibers in cav1-KO lenses. SEM shows the extensive ridge-and-valley membrane surface patterns and dramatic alterations in cell shapes of cortical fiber cells in the cav1-KO lenses at 1 month old as compared with the age-matched wild-type. The dramatic changes of superficial fiber cells (e.g., approximately 50 μm deep) include swelling, irregular shape and smooth cell borders without interlocking protrusions (A). The irregular fiber cells begin to display small number and degree of ridge-and-valleys in outer cortex, approximately 150 μm deep from the lens surface (B). The membranes of fiber cells subsequently undergo a massive formation of extensive ridge-and-valley surface patterns extended toward the entire deep cortical regions (C–F), approximately 600 μm deep from the equatorial lens surface. These extensive ridge-and-valleys are regularly arranged into many elongated bundles with different orientations. They are closely interlocked with those of the neighboring cells, and thus resulting in forming tight intercellular spaces among all surrounding cortical fiber cells. Scale bars: A–F = 1 μm.

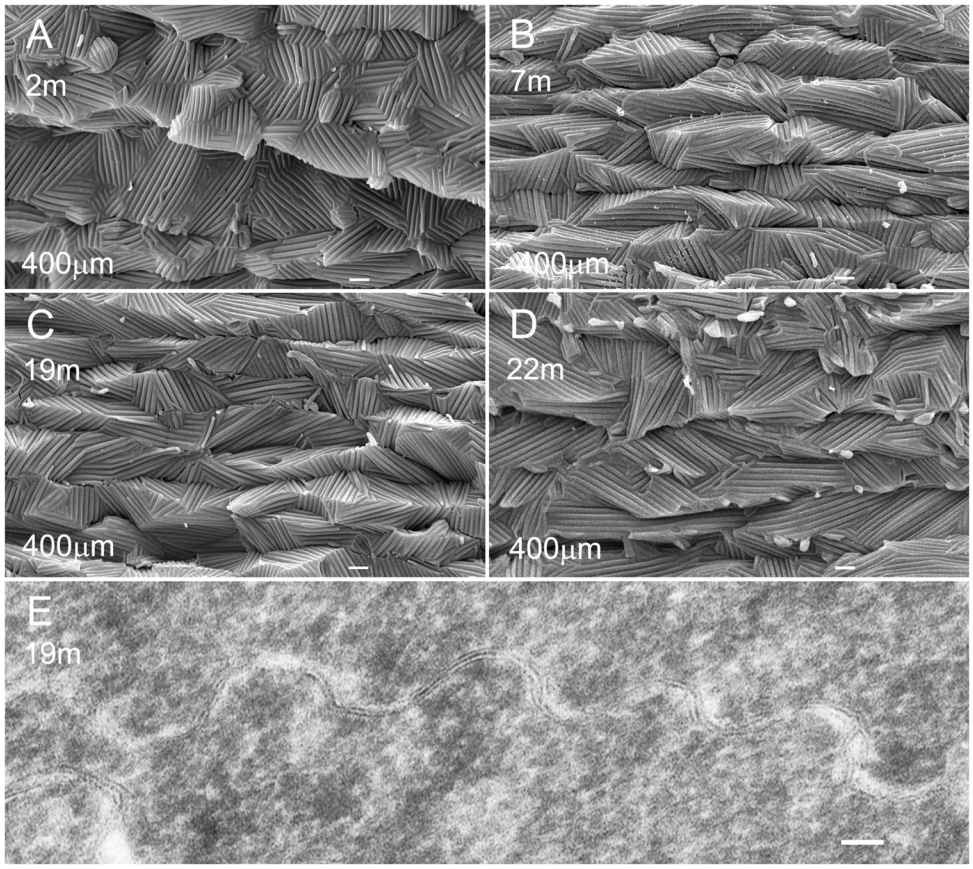

Figure 5.

Similarity of ridge-and-valleys in cortical fibers of cav1-KO lenses at different ages. SEM shows that extensive ridge-and-valleys distributed in 400 μm deep have similar structural configurations in all transparent cortical fibers of cav1-KO mice at 2, 7, 19 and 22 months of age (A to D). The presence of nuclear opacities was found in the 19 and 22 months old lenses. Thin-section TEM reveals the close contact or narrowed extracellular space of the square array junctions between adjacent cortical fiber cells (E). Scale bars: A–D = 1 μm; E= 50 nm.

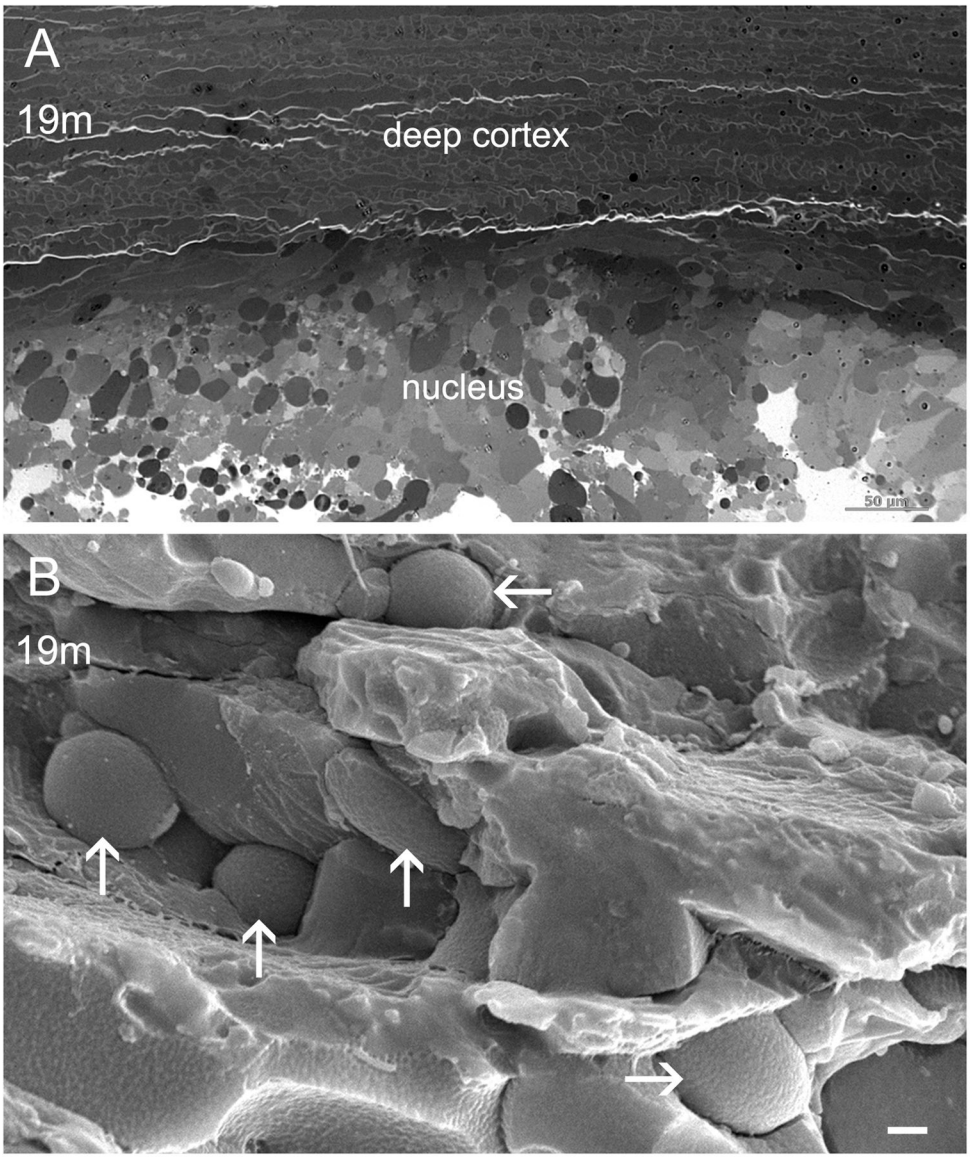

Figure 6.

Cellular breakdown and globule formation in nuclear cataract of aging cav1-KO lens. Thick-section and SEM micrographs (A and B) reveal cellular breakdown and extensive distribution of large globules in the nuclear region of a 19-month-old cav1-KO cataract. Scale bars: A= 50 µm; B= 1 µm.

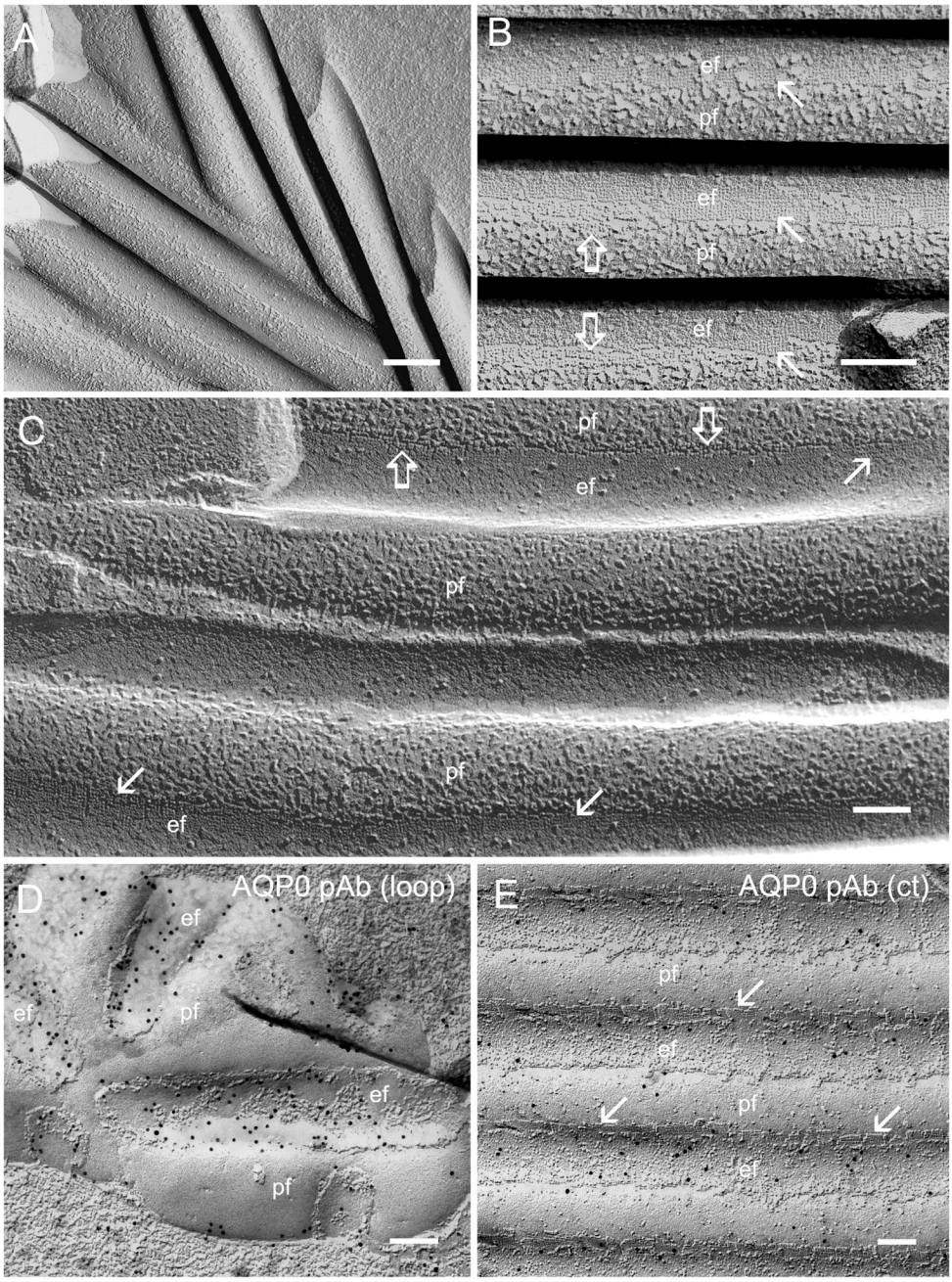

Figure 7.

High resolution structure and immunogold labeling of AQP0-dependant wavy square array junctions. (A) The new wavy square array junctions observed regularly in the outer cortex are arranged into parallel bundles with different orientations. The individual ridge and valley of the parallel bundles are approximately 200 nm in diameter. (B) The square array junctions are visualized as the orthogonal 6.6 nm intramembrane particles (opened arrows) or pits (arrows) at the sides of wavy junctions. (C) This inverted freeze-fracture image is used to ease the visualization of the orthogonal configurations in the e-face pits (arrows) and in the p-face particles (open arrows) of square array junctions. The narrowed intercellular spaces

between the wavy square array junctions are shown concurrently between the p-face and the e-face of the junction membranes (B and C). Many large intramembrane particles (8–9 nm in size) are also distributed on the ridge portions of the wavy junctions. The immunogold labeling of AQP0-loop antibody is regularly seen in wavy square array junctions in the cav1-KO lens (D). In contrast, only a small number of gold particles representing the AQP0-C terminus antibody are distributed on undulating square array junctions in the cav1-KO lens (E). Scale bars:: A = 200 nm; B–E= 100 nm.

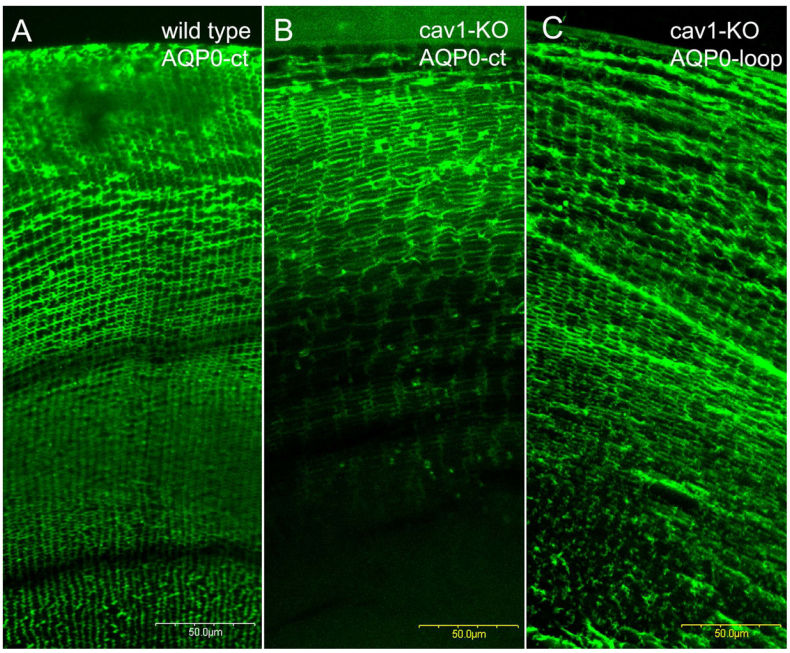

Figure 8.

Immunofluorescence labeling of AQP0 antibodies in wild-type and cav1-KO lenses. The labeling of AQP0-C terminus antibody is seen in the major lens cortex (approximately 300 µm deep) of WT lens (A). In contrast, in the cav1-KO lens the labeling is limited to the more superficial outer cortex (approximately 150 µm deep) (B). By using a polyclonal AQP0-loop antibody, the labeling is seen in the entire outer cortex (C) of the cav1-KO lens. This indicates that premature cleavage of AQP0-C termini occurs in outer cortical fibers of cav1-KO lenses.

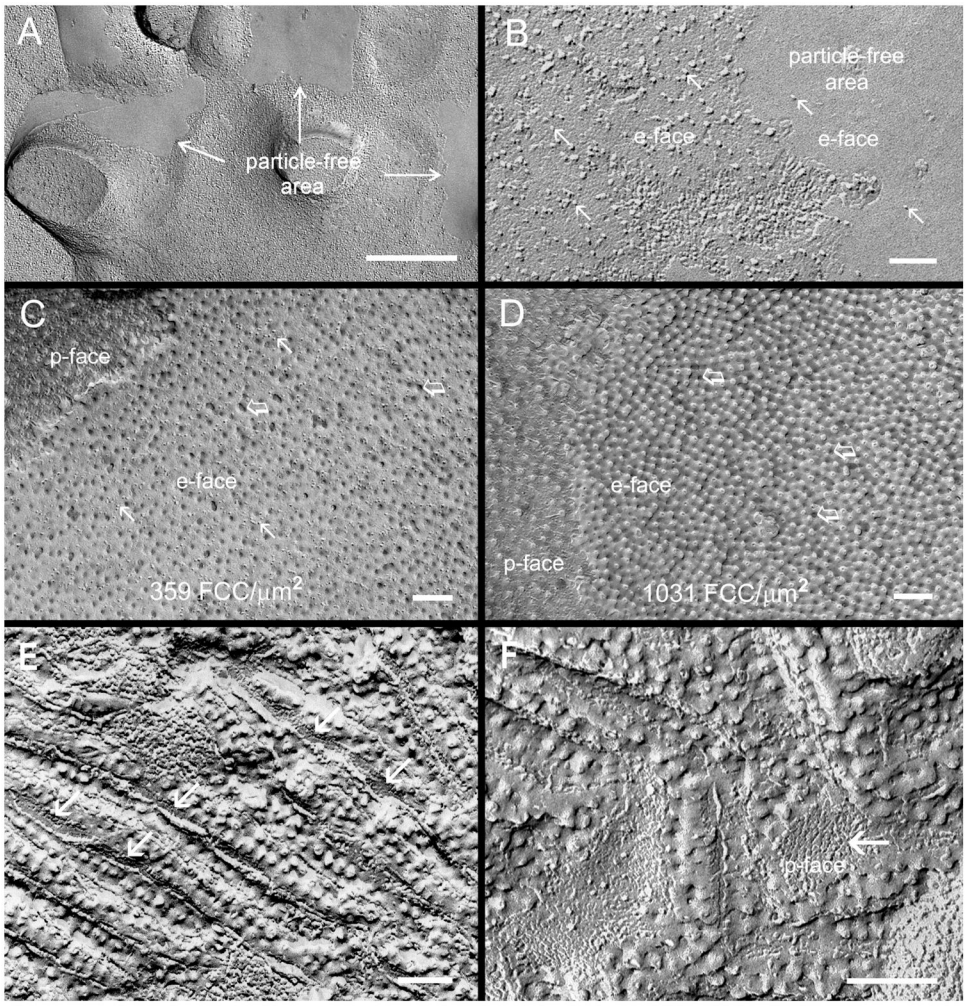

Figure 9.

Filipin cytochemical analysis of membrane cholesterol in cav1-KO lenses. (A and B), The membrane particle free areas are frequently observed in cortical fiber cells in the cav1-KO lenses, suggesting the rich existence of lipid in these membrane areas. At high magnification, only few membrane particles (arrows) are seen on the e-face of the lipid-rich (or particle-free) area (B). This suggests that uneven distribution (mobilization) of membrane protein and lipid may occur in fiber cells of the cav1-KO lens. Filipin cytochemistry analysis indeed reveals that different amounts of filipin-cholesterol-complexes (FCCs) (open arrows) are distributed in the cholesterol-poor (C) and cholesterol-rich area (D). Quantitative estimation indicates that the ratio of cholesterol between the areas of cholesterol-poor (359 FCC/μm^2) and cholesterol-rich (1031 FCC/μm^2) is approximately 1:3. A close examination further shows that many membrane particles (arrows) are distributed on the e-face of cholesterol-poor membrane (C); almost none are found on the e-face of cholesterol-rich membrane (D). In addition, the uneven distribution of cholesterol is also seen in the wavy square array junctions (E and F). The FCCs are mostly distributed on the ridges where the intramembrane particles are few, but are decreased or absent at the

sides or in the valley (arrows) where the intramembrane particles are richly accumulated. Scale bars: A = 500 nm; B–F = 100 nm.